

Upper critical field of $\text{Ba}_{1-x}\text{K}_x\text{BiO}_3$ single crystals

M. Affronte, J. Marcus, and C. Escribe-Filippini

Laboratoire d'Etudes des Propriétés Electroniques des Solides, Centre National de la Recherche Scientifique, Boîte Postale 166, 38042 Grenoble, France

A. Sulpice

Centre de Recherches sur les Très Basses Températures, Centre National de la Recherche Scientifique, Boîte Postale 166, 38042 Grenoble, France

H. Rakoto, J. M. Broto, J. C. Ousset, and S. Askenazy

Laboratoire de Physique des Solides et Service National des Champs Pulsés, 31077 Toulouse, France

A. G. M. Jansen

High Magnetic Field Laboratory, Max-Planck-Institut für Festkörperforschung, Boîte Postale 166, 38042 Grenoble, France

(Received 15 September 1993)

We report an extensive study on the temperature (T) dependence of the upper critical field H_{c2} on $\text{Ba}_{1-x}\text{K}_x\text{BiO}_3$ single crystals. The $H_{c2}(T)$ curve shows a reproducible upward curvature at ~ 22 K. This can be due to the presence of two superconducting phases, one with $T_c \sim 30$ K and low H_{c2} ($[dH_{c2}/dT]_{T_c} \sim 0.5$ T/K) and another one with $T_c \sim 25$ K and higher H_{c2} ($[dH_{c2}/dT]_{T_c} \sim 1.1$ T/K). However, we find that H_{c2} may rise up to 32 T at 1.8 K. It turns out that the reduced critical field $h_{c2} = H_{c2}/[T_c(dH_{c2}/dT)_{T_c}]$ is ≥ 1 at low temperatures for both the 30- and 25-K phases, i.e., much higher than what is expected for a conventional superconductor. We compare the low-temperature h_{c2} data with calculations recently performed by Marsiglio and Carbotte in the framework of an extended Werthamer-Helfand-Hohenberg theory.

INTRODUCTION

The Werthamer-Helfand-Hohenberg¹ (WHH) theory provides a successful description of the upper critical field temperature dependence $H_{c2}(T)$ for most of conventional superconductors. Nevertheless there are several superconductors that show an upward curvature of $H_{c2}(T)$ that is not consistent with the WHH theory. In some cases this upturn is due to the presence of magnetic impurities,² in others to the layered material structure.³ Schossmann and Schachinger⁴ have recently extended the WHH theory including the full electron-phonon interaction. Marsiglio and Carbotte⁵ have found that in the case of large T_c/ω_{in} ratio, where ω_{in} is a characteristic phonon frequency, the $H_{c2}(T)$ curve may actually show an upward curvature. According to this model, the reduced critical field $h_{c2} = H_{c2}/[T_c(dH_{c2}/dT)_{T_c}]$ at zero temperature can be larger than one even in the case of isotropic and nonmagnetic superconductors. This model, however, has been tested only in very few real cases.

$\text{Ba}_{1-x}\text{K}_x\text{BiO}_3$ is a cubic and nonmagnetic material and it has the highest T_c (32 K) among the copper-free superconductors. These features make this material a potential candidate to test the extended WHH theory. It is generally accepted that the electron-phonon coupling plays an important role in this material. However, it is not clear so far whether and how the electron-phonon coupling can account for such relatively high T_c . Early tunneling data⁶⁻⁸ gave a $2\Delta/k_B T_c$ ratio between 3.5 and

3.9 that suggests a moderate electron-phonon coupling ($\lambda \sim 1$). Recent tunneling experiments^{9,10} gave $2\Delta/k_B T_c \sim 4.2$. This is the same value found on Nb_3Sn that has $\lambda \sim 1.8$. It is interesting to analyze different electronic properties in order to see whether $\text{Ba}_{1-x}\text{K}_x\text{BiO}_3$ can be actually considered a conventional weakly coupled superconductor or not.

The upper critical field was measured in $\text{Ba}_{1-x}\text{K}_x\text{BiO}_3$ close to T_c by several groups.¹¹⁻¹⁴ These experiments show a quite small initial slope of the H_{c2} temperature dependence $(dH_{c2}/dT)_{T_c} = 0.5$ T/K. By assuming a conventional $H_{c2}(T)$ behavior a small $H_{c2}(0)$ was predicted for this material (~ 15 T). However, in some experiments¹¹ an anomalous upward curvature of the H_{c2} temperature dependence $H_{c2}(T)$ was observed that reveals a H_{c2} enhancement at low temperatures. No further experiment that extends H_{c2} measurements to lower temperatures has been performed so far.

In this work we present an extensive study on the upper critical field on $\text{Ba}_{1-x}\text{K}_x\text{BiO}_3$ single crystals. We first analyze several structural and physical properties of $\text{Ba}_{1-x}\text{K}_x\text{BiO}_3$ crystals in order to provide information on the sample quality. Crystals used in our experiments were grown by two different methods and they have different quality. However, the presence of microdomains of different phases seems to be a general problem of $\text{Ba}_{1-x}\text{K}_x\text{BiO}_3$ that may affect several physical properties. Samples used in this work are macroscopically single phase. Yet, they have quite different normal-state

transport properties than can be ascribed to the presence of microdomains with different physical properties. We subsequently study the H_{c2} temperature dependence down to 1.8 K in magnetic fields up to 35 T. We found an unconventional temperature dependence of the upper critical field that is, however, well reproducible. We discuss this anomalous behavior on the basis of the characterization done on our crystals. We finally compare the reduced critical field $h_{c2}(0)$ that we evaluate from our measurements with calculations of Marsiglio and Carbotte.⁵

SAMPLE PREPARATION AND CHARACTERIZATION

$\text{Ba}_{1-x}\text{K}_x\text{BiO}_3$ single crystals used in these experiments were grown by two different methods: flux technique (samples *C*) and electrochemical crystallization (samples *A*, *B*, *D*, *E*, and *F*). Samples *D*, *E*, and *F* come from the same batch and we anticipate that they have very similar physical properties. The detailed procedure used for the electrochemical crystallization is reported in Ref. 15. The starting mixture used for the flux growth was KOH, Bi_2O_3 , $\text{Ba}(\text{OH})_2 \cdot 8\text{OH}_2$ in 15:1:2 molar ratio. This mixture was heated at 430 °C in a ZrO_2 crucible.

X-ray-diffraction patterns were taken by a Gandolfi camera. Crystals show a single-phase cubic structure. The width of the x-ray peaks is sharper for crystals *D*, *E*, and *F* than for the other crystals studied. X-ray-spectra refinement gives a lattice parameter of 4.292 ± 0.001 Å with no appreciable differences from sample to sample. According to the relationship between potassium concentration and lattice parameter given in Ref. 16 we evaluated that our crystals have an average potassium content $x = 0.36$. Precession x-ray diffraction shows a mosaic texture of our crystals. In some case it was possible to visualize small misoriented cubes on one side of the main crystal.

The stoichiometric profile was studied by microprobe analysis on several crystals. This analysis was performed on deeply polished surfaces in order to measure the internal stoichiometry. In early batches we often found a gradient of the potassium concentration within the crystals.¹⁵ However, measurements performed on the last series of crystals, from which samples *D*, *E*, and *F* were taken, show that potassium concentration can be considered macroscopically homogeneous within these samples.

Crystals have typical dimensions of $0.4 \times 0.4 \times 0.4$ mm³ and have dark blue color. Two crystals (*E* and *F*) were polished in order to reduce their thickness down to ~ 60 μm.

All crystals are superconducting as grown, i.e., without further heat treatment. Magnetization curves measured in a static field of 10 Oe show the main transition around 30 K. In Fig. 1 we report two characteristic curves measured on crystal *A* and *D*. Sample *A* shows a 10 K broad transition suggesting the presence of slightly different superconducting phases with T_c 's between 20 and 30 K. Sample *D* has one sharp transition at ~ 30 K and a small step at ~ 25 K. This indicates that there are two phases in this crystal, one with $T_c \sim 30$ K and another one with

$T_c \sim 25$ K. It is not clear, however whether such a 25-K transition is due to microdomains spread all over the crystal or to a well localized inclusion. Note that there is no evidence of phases with lower T_c . These results are systematically confirmed by ac susceptibility measurements that we performed on a large number of single crystals. The magnetization value taken during zero-field cooling is generally 100% of the ideal shielding value estimated by using calculated demagnetization factor. The field-cooling signal is typically a few percent of the shielding one and it depends on the pinning properties of different crystals. For example, sample *D* has a Meissner fraction smaller than sample *A* indicating that it has higher pinning energy.

EXPERIMENTAL TECHNIQUES

Four contacts in a van der Pauw configuration were attached on the (100) surface with silver paint. Contacts were annealed at 500 °C for 12 h in oxygen in order to reduce the contact resistance down to ~ 0.5 Ω. This heat treatment did not change the superconducting transition as measured by ac susceptibility. Resistivity and Hall coefficient were evaluated by using standard van der

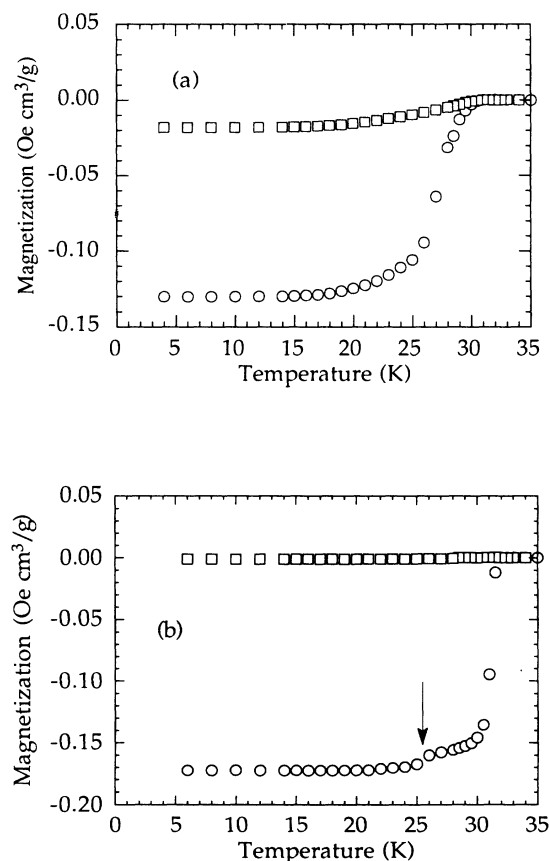


FIG. 1. Zero-field-cooled (circles) and field-cooled (squares) dc magnetization curves measured on $\text{Ba}_{1-x}\text{K}_x\text{BiO}_3$ single crystals. Curves reported in (a) (b) were measured on sample *A* and *D*, respectively. The arrow in (b) shows a second transition occurring at 25 K.

Pauw technique and Montgomery correction factors.

Resistivity, Hall effect, and resistive transition in magnetic field up to 6 T were measured in a standard He flow cryostat inserted in a superconducting coil. Hall measurements were performed by reversing the magnetic field for each temperature.

High magnetic-field measurements were carried out in two laboratories: 20-T Bitter magnet at the High Magnetic Field Laboratory in Grenoble and pulse magnetic fields up to 35 T at the Service National des Champs Pulsés in Toulouse.

For measurements in pulsed magnetic field, resistive transitions were measured by an ac technique (100 kHz) with a selective amplifier and a digital storage triggered by the magnetic field. The increasing and decreasing times of the pulsed magnetic field were 70 and 800 ms, respectively. The resistive signal was recorded during both periods in order to avoid spurious effects such as temperature drift or transient effects. No hysteresis was observed.

In one experiment we applied magnetic field both parallelly and perpendicularly to the crystal plane containing the current. Except for little changes in the shape of the transition, the onset and the foot of the transition are essentially the same for the two magnetic-field orientations. Afterwards we took most of the resistive transitions with the magnetic field within the plane containing the current.

Hall effect and resistive transitions in magnetic fields were measured with currents of typically 1 to 4 mA corresponding to a current density of a few A/cm². No essential changes were observed by decreasing the current by one order of magnitude.

RESISTIVITY AND HALL EFFECT

Ba_{1-x}K_xBiO₃ crystals generally have quite different electronic properties. In Fig. 2 we report the normal-state resistivity of four crystals. Samples *D*, *E*, and *F* show the same behavior, this is why in Fig. 2 we report for simplicity the resistivity of only one of these. We note that in Fig. 2 the resistivity of sample *D* is multiplied by a factor of 10 in order to show it in a proper scale. In

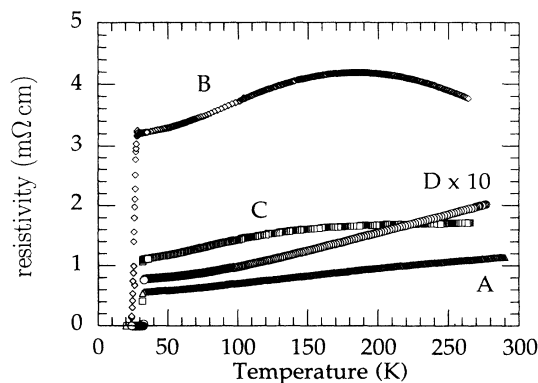


FIG. 2. Temperature dependence of the resistivity measured on crystals *A*, *B*, *C* (data from Ref. 33), and *D*. Note that the resistivity of sample *D* is multiplied by a factor of 10.

Table I we report the resistivity ρ values measured at room temperature and at 40 K, i.e., slightly above the superconducting transition. The room-temperature resistivity $\rho(270\text{ K})$ may range between $\sim 200\text{--}3200\ \mu\Omega\text{ cm}$. Samples with the lowest $\rho(270\text{ K})$ show a metallic temperature dependence of ρ and they have residual resistivity down to $70\ \mu\Omega\text{ cm}$. Sample *B* and *C*, which have higher $\rho(270\text{ K})$, exhibit a bump in the $\rho(T)$ curve. At room temperature the resistivity of sample *B* shows a semiconducting behavior, i.e., the resistivity increases as the temperature decreases. This variety of behavior seems to be typical of this compound and it can be interpreted by a two-component model as was recently proposed by Hellman and Hartford.¹⁷ They showed that the $\rho(T)$ of several Ba_{1-x}K_xBiO₃ thin films can be fitted assuming two resistive contributions, one metallic and another one semiconductorlike. The latter reveals the presence of domains with different potassium and/or oxygen concentration. As macroscopic techniques fail in detecting two different phases, this separation occurs on a microscopic scale and different domains should be intimately mixed. Our data are essentially consistent with this model. However, crystals *D*, *E*, and *F* have $\rho(270\text{ K})$ two times smaller than the most metallic sample reported by Hellman and Hartford and their resistive ratio is $\rho(270\text{ K})/\rho(40\text{ K})\sim 2.6$. These features suggest that the semiconducting component is negligible in crystals *D*, *E*, and *F*. The $\rho(T)$ of these crystals can be fitted by the expression of a purely metallic component:¹⁷

$$\rho_m(T) = \rho_0 + \alpha_m \left[T_{m1} - T_{m2} + T \ln \left| \frac{\exp(T_{m2}/T) - 1}{\exp(T_{m1}/T) - 1} \right| \right].$$

For sample *D*, which is shown in Fig. 2, we found $\rho_0 = 77.85\ \mu\Omega\text{ cm}$, $\alpha_m = 0.8254\ \mu\Omega\text{ cm/K}$, $T_{m1} = 132\text{ K}$, and $T_{m2} = 296\text{ K}$. These values can be compared with $\rho_0 = 220\ \mu\Omega\text{ cm}$, $\alpha_m = 0.96\ \mu\Omega\text{ cm/K}$, $T_{m1} = 120\text{ K}$, and $T_{m2} = 280\text{ K}$ obtained by Hellman and Hartford for their most metallic sample (sample of Ref. 17).

In Fig. 3 we show the temperature dependence of the Hall coefficient R_H measured on four crystals. Again sample *D*, *E*, and *F* have very similar behavior and for simplicity we omit two of them. Hall constant values measured at 270 K are also reported in Table I. We found that R_H of samples *D*, *E*, and *F* is almost one order of magnitude smaller than that measured in sample *C*. Samples with the smallest Hall coefficient also show the most metallic behavior of the resistivity. It is important to note that crystal *D* has the same resistivity and Hall effect than samples *E* and *F* (see Table I) whose thickness was reduced from $\sim 400\ \mu\text{m}$ to $\sim 60\ \mu\text{m}$. This fact corroborates microprobe analysis and it shows that crystals of this batch are macroscopically homogeneous. Samples with higher resistivity (*B* and *C*) have a Hall coefficient that weakly depends on temperature. According to the two-component model we may have an activated contribution at high temperature which is determined by the semiconductorlike phase, while at low temperatures the

TABLE I. Electronic transport properties measured on $\text{Ba}_{1-x}\text{K}_x\text{BiO}_3$ single crystals. The error on the resistivity measurements is $\sim 15\%$. T_c is defined as 10% of the resistive transition.

| Sample numbers | $\rho(270 \text{ K})$ $\mu\Omega \text{ cm}$ | $\rho(40 \text{ K})$ $\mu\Omega \text{ cm}$ | $R_H(270 \text{ K})$ $10^{-9} \text{ m}^3/\text{C}$ | dH_{c2}/dt (T/K) | $H_{c2}(1.8 \text{ K})$ (T) | $T_c^{10\%}$ (K) |
|----------------|-------------------------------------------------|------------------------------------------------|--------------------------------------------------------|-----------------------|--------------------------------|------------------|
| A | 1110 | 570 | -1.22 ± 0.2 | -0.55 ± 0.10 | | 30.1 |
| B | 3750 | 3170 | -2.73 ± 0.5 | -0.65 ± 0.10 | | 24.5 |
| C | 1710 | 1150 | -3.36 ± 0.7 | -0.64 ± 0.10 | 32 | 28.1 |
| D | 202 | 79 | -0.69 ± 0.15 | -0.51 ± 0.10 | | 28.9 |
| E | 237 | 92 | -0.64 ± 0.15 | -0.55 ± 0.10 | 25 | 28.8 |
| F | 198 | 72 | -0.56 ± 0.15 | -0.56 ± 0.10 | | 28.0 |

metallic component dominates and the Hall coefficient is essentially temperature independent.¹⁷ However in the most metallic samples (*D*, *E*, and *F*) we found that the Hall coefficient is temperature independent. This confirms that the semiconducting component is not active in these crystals, consistently with the resistivity behavior. A temperature-independent Hall coefficient is quite interesting as compared to the anomalous temperature dependence observed on most of the high- T_c superconducting oxides. Hall data can be combined with resistivity in order to get the cotangent of the Hall angle $\cot\Theta_H$. For some cuprates it was found that $\cot\Theta_H$ has a quadratic temperature dependence. This was ascribed to the presence of exotic spin excitations.¹⁸ However it was shown that it can also be interpreted within the framework of the Fermi-liquid theory by assuming a nonspherical Fermi surface.^{19,20} Although this controversy is still quite open, it is reassuring to find that a cubic and non-magnetic perovskite, such as $\text{Ba}_{1-x}\text{K}_x\text{BiO}_3$, behaves like an ordinary metal.

Electronic band calculations performed by Hamada *et al.*²¹ showed that only one band is present at the Fermi surface. Assuming a simple Drude model² we can estimate some characteristic electronic properties of this compound that we summarize in Table II. Note that the characteristic quantities are calculated assuming the presence of only the homogeneous metallic phase.

Briefly, we conclude from the set of data presented so far that our crystals can be considered macroscopically

homogeneous and they contain a majority phase with $T_c \sim 30 \text{ K}$. The analysis of normal-state transport properties shows, however, that crystals *A*, *B*, and *C* contain microdomains of a semiconducting phase. This phase seems to be not present on crystals *D*, *E*, and *F*. Furthermore, based on susceptibility measurements performed on a large number of crystals, we suspect that our crystals may contain microdomains of a second superconducting phase with $T_c \sim 25 \text{ K}$. According to the phase diagram reported by Pei *et al.*¹⁶ the 30-K phase is $\text{Ba}_{0.65}\text{K}_{0.35}\text{BiO}_3$, while the semiconducting and the 25-K phases should be, respectively, poorer and richer in potassium.

MEASUREMENTS IN HIGH MAGNETIC FIELDS

One of the main features of the normal-state resistivity shown in Fig. 2 is the fact that it saturates at low temperature. Such behavior is not observed in most of the superconducting oxides. In order to further investigate this point we measure the low-temperature resistivity of one sample in a static field of 20 T. The result is reported in Fig. 4 and it can be compared with data taken in zero field. Notice that above 30 K the magnetoresistance at 20 T is very small and it cannot be measured with our experimental accuracy. Therefore the two curves, at zero and 20 T, overlap between 30 and 40 K. Below T_c the curve taken in magnetic field extends well the normal-state behavior.

In Fig. 5 we report some resistive transitions taken in quasistatic magnetic fields up to 20 T. Similar curves were obtained in pulsed magnetic fields and they are reported in Ref. 23. There are two main features worth mentioning: Transitions are very sharp close to $\sim 30 \text{ K}$. As the temperature decreases they are bodily shifted towards higher fields and they slightly broaden. This behavior is very similar to that shown by conventional superconductors and it is quite different to what is observed on most of the high- T_c superconducting oxides. These exhibit very broad transitions in magnetic field. Another important feature of the curves reported in Fig. 5 is the fact that the resistance saturates for high enough magnetic-field strength. All the curves saturate to the same value. This is not surprising because, as we have shown before, the normal-state resistivity is temperature independent below $\sim 50 \text{ K}$.

The huge broadening of the resistive transition ob-

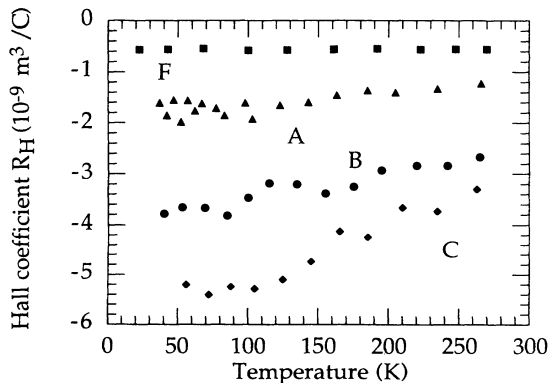


FIG. 3. Temperature dependence of the Hall coefficient measured on crystals *A*, *B*, *C* (data from Ref. 33), and *F*.

TABLE II. Characteristic electronic properties of $\text{Ba}_{1-x}\text{K}_x\text{BiO}_3$ evaluated within the framework of the Drude model (Ref. 22). Resistivity, resistivity slope α , and Hall coefficient are typical values measured on our most metallic samples (*D*, *E*, and *F*). The resistivity ρ is expressed in $\mu\Omega$ cm. The upper critical field H_{c2} (1.8 K) was measured on sample *C*. The electron-phonon coupling constant was evaluated by using the formula given by M. Gurvitch, *Physica B* **135**, 276 (1985).

| | | |
|---------------------------------------------|------------------------------------------------------------------------------|-------------------------------------------|
| Resistivity | $\rho(270 \text{ K})$ | 200 $\mu\Omega$ cm |
| | $\rho(40 \text{ K})$ | 80 $\mu\Omega$ cm |
| Resistivity Slope | $\alpha(250 \text{ K})=d\rho/dT$ | 0.6 $\mu\Omega$ cm/K |
| Hall coefficient | R_H | $0.6 \times 10^{-9} \text{ m}^3/\text{C}$ |
| Hall number | $n_H=1/eR_H$ | $1.04 \times 10^{22} \text{ cm}^{-3}$ |
| Unit cell volume | V | 78.4 \AA^3 |
| Electron density per unit cell | n_0 | 0.81 \bar{z} /unit cell |
| Radius of the sphere occupied by 1 electron | $r_s/a_0=5.44x(n_H[10^{22}\text{cm}^{-3}])^{-1/3}$ ($a_0=\hbar^2/me^2$) | 5.37 |
| Plasma energy | $\hbar\omega_p=47.1[\text{eV}] \times (r_s/a_0)^{-3/2}$ | 3.79 eV |
| Electron-phonon coupling constant | $\lambda=0.246(\hbar\omega_p)^2\alpha$ | 1.7 to 2.1 |
| Electron relation time | $\tau(40 \text{ K})=2.2 \times 10^{-15}[\text{s}] \times (r_s/a_0)^3/\rho$ | $4.26 \times 10^{-15} \text{ s}$ |
| Impurity parameter | $t^+ \sim \hbar/2\pi\tau$ | 0.15 eV |
| Mean free path | $l(40 \text{ K})=[92 \text{ \AA}][(r_s/a_0)^{-2}/\rho]$ | 33 \AA |
| Upper critical field | $H_{c2}(1.8 \text{ K})$ | 32 T |
| Paramagnetic critical field | $H_p=1.84T_c$ | 55 T |
| Coherence length | $\xi=(\phi_0/2\pi H_{c2})^{1/2}$ | 32 \AA |

served in high- T_c superconductors has been discussed by several authors.^{24–26} It is generally accepted that the foot of the transition is determined by a (flux-creep) thermally activated process. High- T_c superconductors are characterized by very low pinning energies U_0 (~ 0.1 eV) and high T_c (~ 90 K). This implies that the $U_0/k_B T_c$ ratio is particularly small (~ 10) and therefore thermally activated phenomena are particularly important in these materials. Malozemoff *et al.*²⁵ pointed out an important consequence of this fact. They argued that, in the case of small $U_0/k_B T$, transport measurements determine the irreversibility line rather than the thermodynamic critical field H_{c2} . Magnetic measurements¹⁴ have shown the presence of an irreversibility line which lies below the H_{c2} curve

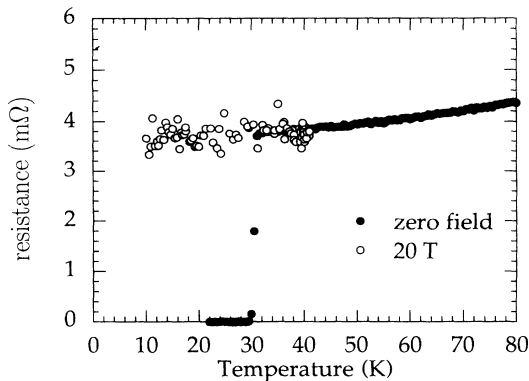


FIG. 4. Low-temperature resistance of sample *A* measured in zero field and 20 T.

also in the case of $\text{Ba}_{1-x}\text{K}_x\text{BiO}_3$. So one may wonder whether resistivity measurements are a good method to determine H_{c2} for $\text{Ba}_{1-x}\text{K}_x\text{BiO}_3$. Seidler *et al.*¹⁴ have found by magnetization measurements the characteristic pinning energy $U_0=0.26$ eV in $\text{Ba}_{1-x}\text{K}_x\text{BiO}_3$ single crystals. By plotting the foot of the resistive transition ($10^{-6} < \rho/\rho_0 < 10^{-3}$) in magnetic field in an Arrhenius plot, as suggested by Palstra *et al.*,²⁷ we have also evaluated the pinning energy. Preliminary results give a temperature- and field-dependent U whose value is somewhat higher than that found by Seidler *et al.*¹⁴ At 2.5

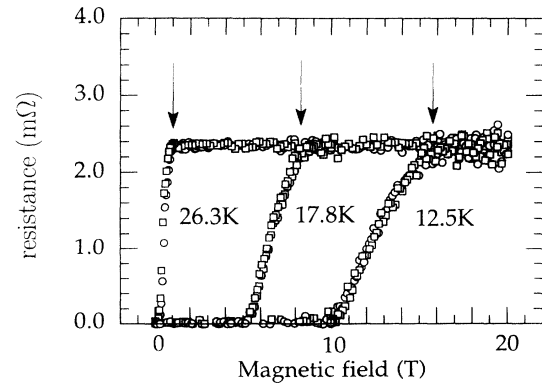


FIG. 5. Resistive transitions measured in quasistatic magnetic field at different temperatures: 26.3, 17.8, and 12.5 K. The squares show the curve taken with an increasing field, while circles show that with decreasing field for each temperature. They can be hardly distinguished. Arrows show the upper critical field according to the definition given in the text.

kOe and 26 K we find $U=0.52$ eV. A larger activation energy as compared to that of cuprates is not surprising because of the isotropic structure and the longer coherence length of $\text{Ba}_{1-x}\text{K}_x\text{BiO}_3$. As $T_c \sim 30$ K, it turns out that the $U_0/k_B T_c$ ratio is greater than 100 in this material. Following the argument given by Malozemoff *et al.*,²⁵ if we simply take, for example, the foot of the resistive transition to determine H_{c2} this would differ from a thermodynamically determined H_{c2} by less than $\sim 20\%$. However, we define the upper critical field H_{c2} as the onset of the resistive transition, i.e., the field required to achieve the resistivity saturation. This definition is certainly more suitable in order to avoid any complication given by the flux motion.²⁵ We note, however, that a different choice of the H_{c2} definition does not change the $H_{c2}(T)$ shape.

We first studied the behavior of the upper critical field H_{c2} near T_c . In Fig. 6 we report the temperature dependence of H_{c2} measured on crystal *E*. It can be compared with magnetic¹⁴ and specific-heat¹³ measurements reported in the literature. This plot shows that, except for the slightly different T_c of the samples, the H_{c2} behavior is very similar in these experiments. Very close to T_c the H_{c2} has a linear temperature dependence and the $H_{c2}(T)$ slope near T_c , $(dH_{c2}/dT)_{T_c}$, is also very similar. Notice that a linear temperature dependence near T_c is in agreement with the thermodynamic considerations based on the Ginzburg-Landau theory of the upper critical field and it differs to the power-law dependence $(1-T/T_c)^p \sim H$ typical of the irreversibility line. In Table I we reported the $(dH_{c2}/dT)_{T_c}$ values that we measured in different crystals. We found that $(dH_{c2}/dT)_{T_c}$ ranges between 0.51–0.65 T/K in our samples. These values are in good agreement with data reported in the literature and obtained by different methods and on different samples.^{11–14} The agreement between resistive and thermodynamic measurements confirms that dissipa-

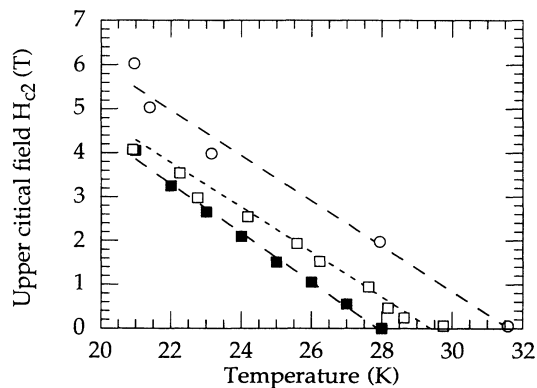


FIG. 6. Upper critical field near T_c measured on $\text{Ba}_{1-x}\text{K}_x\text{BiO}_3$ single crystals. Filled squares are resistive measurements taken on crystal *E*. Empty squares are magnetization measurements taken from Ref. 14. Empty circles are specific heat measurements taken from Ref. 13. Except for the different T_c these crystals show very similar H_{c2} behavior.

tion effects do not affect the H_{c2} determination in $\text{Ba}_{1-x}\text{K}_x\text{BiO}_3$.¹¹ We also note that for YBCO and other high- T_c superconducting oxides $(dH_{c2}/dT)_{T_c}$ is at least one order of magnitude greater.

The whole temperature dependence of the upper critical field measured in our samples is reported in Figs. 7(a) and 7(b). One important feature of these data is the fact that at low temperatures the upper critical field H_{c2} is very high. At 1.8 K we measured $H_{c2}=32$ T on sample *C* and 25 T on sample *E*. With $H_{c2}(0)=32$ T we get a coherence length $\xi=(\phi_0/2\pi H_{c2})^{1/2}=32$ Å ($\phi_0=2.07\times 10^{-15}$ T m²). Data obtained in quasistatic field confirmed that below ~ 8 K the normal state was not achieved for a magnetic field of 20 T in all the samples we studied. We just mention here that we have also performed tunneling measurement in high magnetic field in one $\text{Ba}_{1-x}\text{K}_x\text{BiO}_3$ crystal of the same batch as samples *D*, *E*, and *F*.¹⁰ We found that at 4.2 K it is still superconducting in a magnetic field of 20 T. As tunneling measurements are not affected by dissipation phenomena this result confirms that H_{c2} is certainly higher than 20 T at liquid-He temperatures.

Near ~ 22 K, the $H_{c2}(T)$ curve shows an upward curvature. This upturn is observed in all the crystals we

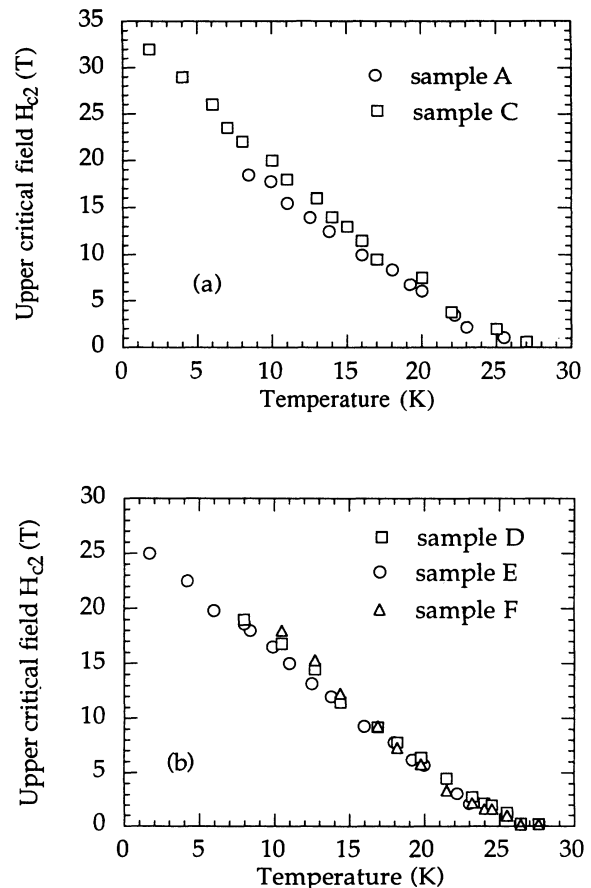


FIG. 7. Temperature dependence of the upper critical field measured on $\text{Ba}_{1-x}\text{K}_x\text{BiO}_3$ single crystals. The upward curvature of the $H_{c2}(T)$ curve is observed in all our crystals. Data of sample *C* are taken from Ref. 23.

studied independently of their normal-state properties. In Fig. 8 we plot the reduced critical field h_{c2} as a function of the normalized temperature $t = T/T_c$ for crystals *C* and *E*. Despite these crystals have quite different normal-state properties, they exhibit a very similar h_{c2} behavior. Below ~ 20 K the H_{c2} temperature dependence is approximately linear down to 1.8 K, the lowest temperature we attained. In particular, we do not observe any clear change of the slope of the $H_{c2}(T)$ curve between ~ 20 and 1.8 K. Moreover, we do not observe any saturation of the $H_{c2}(T)$ curve at low temperatures.

DISCUSSION

Based on the analysis of the structural and normal-state transport properties, we first discuss possible effects due to the presence of different phases. In Fig. 8 we show that crystals *C* and *E* have almost identical $h_{c2}(t)$ behavior although the normal-state properties of crystal *E* are purely metallic, while those of crystal *C* reveal the presence of semiconducting domains. We conclude that the semiconducting phase does not play an important role in the determination of the upper critical-field behavior. On the other hand, we may assume that $\text{Ba}_{1-x}\text{K}_x\text{BiO}_3$ crystals are made of two superconducting phases. On the basis of susceptibility measurements, we take one phase with $T_c \sim 30$ K and another one with $T_c \sim 25$ K. The slope of the $H_{c2}(T)$ curve $(dH_{c2}/dT)_{T_c}$ measured above 23 K belongs to the 30-K phase. Assuming a conventional behavior we may guess the low-temperature behavior of this phase. We get

$$H_{c2}(0) = 0.693 \times T_c \times (dH_{c2}/dT)_{T_c} = 10.7 \text{ T}$$

at which it corresponds a coherence length $\xi = 55 \text{ \AA}$. Below ~ 22 K the low-temperature phase dominates and it determines the H_{c2} behavior. Taking $T_c \sim 25$ K, we try to fit the H_{c2} behavior with a conventional WHH curve. The 25-K phase has a $H_{c2}(T)$ initial slope $(dH_{c2}/dT)_{T_c} = 1.1 \text{ T/K}$ and using standard formula we get

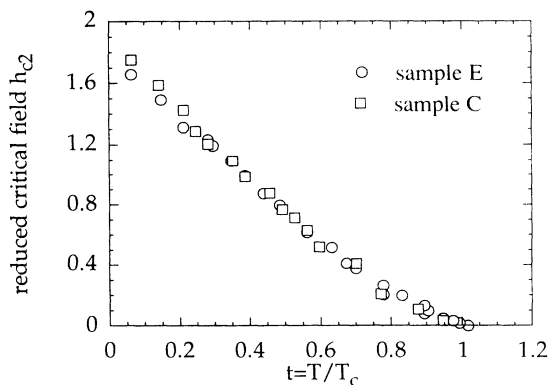


FIG. 8. Reduced critical field $h_{c2} = H_{c2}/[T_c(dH_{c2}/dT)_{T_c}]$ as a function of the reduced temperature $t = T/T_c$ measured on samples *C* and *E*.

$$H_{c2}(0) = 0.693 \times T_c \times (dH_{c2}/dT)_{T_c} = 18.3 \text{ T}$$

that gives $\xi = 42 \text{ \AA}$. This two-phase model may apply either in the case of spatially separated domains with different potassium concentration or in the case of structural phase transition occurring below T_c . Marx *et al.*²⁸ have actually found that the related BaPbBiO system is metastable. However, Fleming *et al.*²⁹ did not find any structural transition in $\text{Ba}_{1-x}\text{K}_x\text{BiO}_3$ between 14 and 300 K. According to the conventional H_{c2} theory, $H_{c2}(0)$ is proportional to $(T_c/\nu_F)^2$ in the clean limit and to $T_c/\tau\nu_F^2$ in the dirty limit— ν_F is the Fermi velocity and τ the scattering rate. As $\text{Ba}_{1-x}\text{K}_x\text{BiO}_3$ is in the intermediate regime (see Table II), the $H_{c2}(0)$ is essentially a combination of these two expressions. Thus we may have higher H_{c2} in a low- T_c phase if ν_F or τ are much smaller in this phase as compared to those of the plane with higher T_c . In the case of $\text{Ba}_{1-x}\text{K}_x\text{BiO}_3$ we may actually have one phase with $T_c \sim 30$ K and potassium concentration $x \sim 0.35$ and a 25-K phase with higher potassium concentration, let us say $x \sim 0.45$. In a naive chemical model, potassium doping is expected to reduce the density of electron in $\text{Ba}_{1-x}\text{K}_x\text{BiO}_3$. As $\text{Ba}_{1-x}\text{K}_x\text{BiO}_3$ is an electron-doped system, the K-rich phase would have a lower Fermi energy and this could explain the higher upper critical field as compared to the 30-K phase.

In Fig. 9 we plot the H_{c2} temperature dependence of crystal *E* with the two conventional curves related to the 30 and 25-K phases. It is clear from this plot that this two-phase model may actually account for data above ~ 12 K. Yet, at low temperatures H_{c2} increases much more than what is expected for a conventional 25-K superconductor. We may assume the presence of a third phase with $T_c \sim 15$ K and $H_{c2}(0) \sim 25$ –30 T. However, we have never found evidence of 15-K phase in susceptibility measurements in our single crystals. Furthermore, according to the phase diagram reported by Pei *et al.*¹⁶ all the superconducting phases of $\text{Ba}_{1-x}\text{K}_x\text{BiO}_3$ have T_c higher than 20 K. Thus the existence of the 15-K phase is not supported by other measurements.

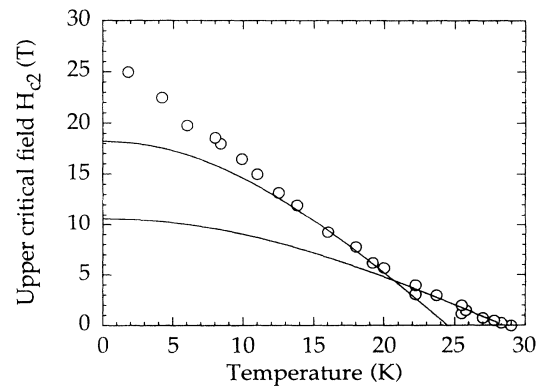


FIG. 9. Temperature dependence of the upper critical field measured on sample *E* (circles). The two unbroken curves show the conventional WHH behavior expected for a 30- and a 25-K superconductor, respectively. The initial slope of these curves was chosen to fit the experimental data.

Based on these considerations, we believe that the anomalous H_{c2} increase observed at low temperatures is not an artifact due to presence of different phases, but it has to be considered as a genuine feature of one single phase. In the following we shall discuss the origin of this enhancement.

We first note that we cannot ascribe the low temperature H_{c2} enhancement either to magnetic pair-breaking mechanism or to effects related to anisotropy, since $\text{Ba}_{1-x}\text{K}_x\text{BiO}_3$ is a cubic and nonmagnetic material. We also note that the Clogston paramagnetic limit $H_p = 1.84 \times T_c$ is 55 T for $\text{Ba}_{1-x}\text{K}_x\text{BiO}_3$ (see Table II). That is much higher than the measured H_{c2} . Accordingly, we expect that spin paramagnetic effects should be unimportant in this material.

As $\text{Ba}_{1-x}\text{K}_x\text{BiO}_3$ generally exhibits a rather conventional behavior, it is interesting to see to what extent the BCS-derived theories are able to describe the temperature dependence of the upper critical field. The Werthamer-Helfand-Hohenberg (WHH) theory¹ predicts a linear temperature dependence of H_{c2} near T_c and a downward curvature at lower temperatures. We have shown that, even if two phases are presented in $\text{Ba}_{1-x}\text{K}_x\text{BiO}_3$ crystals, this theory is not able to account for the low-temperature H_{c2} behavior of $\text{Ba}_{1-x}\text{K}_x\text{BiO}_3$. Schossmann and Schachinger⁴ have recently extended the WHH theory including the full electron-phonon interaction. Based on the $H_{c2}(T)$ expression given by Schossmann and Schachinger, Marsiglio and Carbotte⁵ and independently Bulaevskii and Dolgov³⁰ have found that the $H_{c2}(T)$ curve may actually show a positive curvature in the middle range of temperature in the case of large T_c/ω_{in} ratio and the reduced critical field $h_{c2}(0) = H_{c2}(0)/[T_c(dH_{c2}/dT)_{T_c}]$ can be larger than 1 in this case. The logarithmic mean phonon frequency ω_{in} is defined as

$$\omega_{\text{in}} = \exp \left[\frac{2}{\lambda} \int_0^\infty \frac{\alpha^2 F(\omega)}{\omega} \ln(\omega) d\omega \right],$$

where $\alpha^2 F(\omega)$ is the Eliashberg function and λ is the electron-phonon coupling constant. Marsiglio and Carbotte have shown that the temperature dependence of h_{c2} weakly depends on the shape of the phonon spectra. For example, they found that the $h_{c2}(t)$ curve calculated using the phonon spectra of Pb and LaSrCuO are quite similar and they depend on the electron-phonon coupling strength and on the specimen purity. Thus, in first approximation, $h_{c2}(t)$ can be expressed in terms of two parameters: the T_c/ω_{in} ratio and the impurity parameter $t^+ = h/2\pi\tau$. In order to compare our data with these calculations, it is convenient to measure the reduced critical field. If the observed low-temperature H_{c2} is given by one single phase with $T_c \sim 30$ K, we have $h_{c2}(0) \sim 1.7$ (see

Fig. 8), that is more than twice the conventional WHH value. According to calculations of Marsiglio and Carbotte (see Fig. 3 of Ref. 5) it turns out that it would require $T_c/\omega_{\text{in}} \sim 1$ and $t^+ \geq 100$ meV in order to have $h_{c2}(0) \sim 1.7$. Note that for our most metallic samples we found $t^+ \sim 150$ meV (see Table II). On the basis of the previous discussion, however, we can ascribe the low temperatures H_{c2} behavior to a superconducting phase with $T_c = 25$ K as well. In this case we have $h_{c2}(0) \sim 1$, a value that is still larger than the conventional one. According to calculations of Marsiglio and Carbotte it requires $T_c/\omega_{\text{in}} = 0.4$ and $t^+ \geq 0$ in order to have $h_{c2}(0) \sim 1$. It is worth noting that most of conventional superconductors have a T_c/ω_{in} ratio that is not greater than 0.25.³¹ Moreover, ω_{in} , λ , and T_c are not independent quantities but they are closely related in the extended WHH theory.³¹ Note, for example, that using standard expressions, $T_c/\omega_{\text{in}} \geq 0.4$ would correspond to a huge λ value.³¹ Both the electron-phonon coupling constant λ and ω_{in} are determined by the Eliashberg function $\alpha^2 F(\omega)$. Although the second derivative of tunneling measurements reproduces some of the structures found in neutron-scattering measurements,³² the detailed shape of $\alpha^2 F(\omega)$ obtained by tunneling measurements is, so far, sample dependent.⁷⁻⁹ So the $\alpha^2 F(\omega)$ function is not known with enough accuracy for an unambiguous determination of λ and ω_{in} in $\text{Ba}_{1-x}\text{K}_x\text{BiO}_3$. We shall not speculate on the different possibilities to combine T_c , ω_{in} , and λ . We rather conclude from our experiments that $\text{Ba}_{1-x}\text{K}_x\text{BiO}_3$ cannot be simply considered as a conventional weakly coupled superconductor.

In conclusion, we measured the temperature dependence of the upper critical field in several $\text{Ba}_{1-x}\text{K}_x\text{BiO}_3$ crystals. We found that the H_{c2} temperature dependence shows a reproducible upward curvature close to 22 K that can be ascribed to the presence of two different phases, one with $T_c \sim 30$ K and another one with $T_c \sim 25$ K. However, below 20 K H_{c2} follows an approximately linear dependence with no saturation down to 1.8 K, a quite different behavior as compared to what is expected for a conventional superconductor. We compare the reduced field $h_{c2}(0)$ of the 30 and 25-K phases with calculations of Marsiglio and Carbotte. Within the framework of this model, it turns out that $\text{Ba}_{1-x}\text{K}_x\text{BiO}_3$ is characterized by a T_c/ω_{in} ratio greater than 0.4.

ACKNOWLEDGMENTS

This work was partially supported by the Commission of the European Communities Contract No. SCI*CT92-0785. X-ray studies were done by C. Chailout that we gratefully acknowledge. We thank F. Cyrot-Lackmann and M. Cyrot who stimulated studies on copper-free superconducting oxides and C. Cappoen who collaborated to sample preparation. We also thank B. K. Chakraverty, A. Taraphder, D. Feinberg, D. Mayou, and J. P. Julien for stimulating discussions.

- ¹N. R. Werthamer, E. Helfand, and P. C. Hohenberg, *Phys. Rev.* **147**, 295 (1966).
- ²Ø. Fischer, M. Decroux, S. Roth, R. Chevrel, and M. Sergent, *J. Phys. C* **8**, L474 (1975).
- ³R. A. Klemm, A. Luther, and R. M. Beasley, *Phys. Rev. B* **12**, 877 (1975); D. E. Prober, R. E. Schwall, and R. M. Beasley, *ibid.* **21**, 2717 (1980).
- ⁴M. Schossmann and E. Schachinger, *Phys. Rev. B* **33**, 6123 (1986).
- ⁵F. Marsiglio and J. P. Carbotte, *Phys. Rev. B* **36**, 3633 (1987).
- ⁶H. Sato, H. Takagi, and S. Uchida, *Physica C* **169**, 391 (1990).
- ⁷J. F. Zasadzinski, N. Tralshawala, D. G. Hinks, B. Dabrowski, A. W. Mitchell, and D. R. Richards, *Physica C* **158**, 519 (1989).
- ⁸Q. Huang, J. F. Zasadzinski, N. Tralshawala, K. E. Gray, D. G. Hinks, J. L. Peng, and R. L. Greene, *Nature (London)* **347**, 369 (1990).
- ⁹P. Samuely, N. L. Bobrov, A. G. M. Jansen, P. Wyder, S. N. Barilo, and S. V. Shiryayev, *Phys. Rev. B* **48**, 13 904 (1993).
- ¹⁰P. Samuely, P. Szabó, A. G. M. Jansen, P. Wyder, J. Marcus, C. Escribe-Filippini, and M. Affronte, *Physica B* (to be published).
- ¹¹W. K. Kwok, U. Welp, G. W. Crabtree, K. G. Vandervoort, R. Hulscher, Y. Zheng, B. Dabrowski, and D. G. Hinks, *Phys. Rev. B* **40**, 9400 (1989).
- ¹²I. Tomeno and K. Ando, *Phys. Rev. B* **40**, 2690 (1989).
- ¹³J. E. Graebner, L. F. Schneemeyer, and J. K. Thomas, *Phys. Rev. B* **39**, 9682 (1989).
- ¹⁴G. T. Seidler, T. F. Rosebaum, P. D. Han, D. A. Payne, and B. W. Veal, *Physica C* **195**, 373 (1992).
- ¹⁵J. Marcus, C. Escribe-Filippini, S. K. Agarwal, C. Chaillout, J. Durr, T. Fournier, and J. L. Tholence, *Solid State Commun.* **78**, 967 (1991).
- ¹⁶S. Pei, J. D. Jorgensen, B. Dabrowski, D. G. Hinks, D. R. Richards, A. W. Mitchell, J. M. Newsam, S. K. Sinha, D. Sinha, D. Vakin, and A. J. Jacobson, *Phys. Rev. B* **41**, 4126 (1990).
- ¹⁷E. S. Hellman and E. H. Hartford, *Phys. Rev. B* **47**, 11 346 (1993).
- ¹⁸P. W. Anderson, *Phys. Rev. Lett.* **67**, 2992 (1991).
- ¹⁹A. Carrington, A. P. Mackenzie, C. T. Lin, and J. R. Cooper, *Phys. Rev. Lett.* **69**, 2855 (1992).
- ²⁰C. Kenziora, D. Mandrus, L. Mihaly, and L. Forro, *Phys. Rev. B* **46**, 14 297 (1992).
- ²¹N. Hamada, S. Massidda, A. J. Freeman, and J. Redinger, *Phys. Rev. B* **40**, 4442 (1989).
- ²²N. W. Ashcroft and N. D. Mermin, *Solid State Physics* (Saunders, Philadelphia, 1976).
- ²³C. Escribe-Filippini, J. Marcus, M. Affronte, H. Rakoto, J. M. Broto, J. C. Ousset, and S. Askenazy, *Physica C* **210**, 133 (1993).
- ²⁴K. A. Müller, M. Takashige, and J. G. Bednorz, *Phys. Rev. Lett.* **58**, 1143 (1987).
- ²⁵A. P. Malozemoff, T. K. Worthington, Y. Yeshurun, F. Holtzberg, and P. H. Kes, *Phys. Rev. B* **38**, 7203 (1988); Y. Yeshurun and A. P. Malozemoff, *Phys. Rev. Lett.* **60**, 2202 (1988).
- ²⁶M. Tinkham, *Phys. Rev. Lett.* **14**, 1658 (1988).
- ²⁷T. T. M. Palstra, B. Batlogg, L. F. Schneemeyer, and J. V. Waszczak, *Phys. Rev. Lett.* **61**, 1662 (1988).
- ²⁸D. T. Marx, P. G. Radaelli, J. D. Jorgensen, R. L. Hitterman, D. G. Hinks, S. Pei, and B. Dabrowski, *Phys. Rev. B* **46**, 1144 (1992).
- ²⁹R. M. Fleming, P. Marsh, R. J. Cava, and J. J. Krajewski, *Phys. Rev. B* **38**, 7026 (1988).
- ³⁰L. N. Bulaevskii and O. V. Dolgov, *Pis'ma Zh. Eksp. Teor. Fiz.* **45**, 413 (1987) [*JETP Lett.* **45**, 526 (1987)].
- ³¹J. P. Carbotte, *Rev. Mod. Phys.* **62**, 1027 (1990).
- ³²C. K. Loong, P. Vashishta, R. K. Kalia, M. H. Degani, D. L. Price, J. D. Jorgensen, D. G. Hinks, B. Dabrowski, A. W. Mitchell, D. R. Richards, and Y. Zheng, *Phys. Rev. Lett.* **62**, 2628 (1989).
- ³³M. Affronte, J. Marcus, and C. Escribe-Filippini, *Solid State Commun.* **85**, 501 (1993).